Zhang YL, Zhang J, Jiang N et al.Immunosuppressive polyketides from mantis-associated Daldinia eschscholzii. J Am Chem Soc 133:5931-5940

ARTICLE *in* JOURNAL OF THE AMERICAN CHEMICAL SOCIETY · MARCH 2011

Impact Factor: 12.11 · DOI: 10.1021/ja110932p · Source: PubMed

JACS
JOURNAL OF THE AMERICAN CHEMICAL SOCIETY

ARTICLE

pubs.acs.org/JACS

Immunosuppressive Polyketides from Mantis-Associated *Daldinia eschscholzii*

Ying L. Zhang,[#,†,§] Jie Zhang,[#,†] Nan Jiang,[‡] Yan H. Lu,[∥] Lu Wang,[†] Su H. Xu,[†] Wei Wang,[†] Gao F. Zhang,[†] Qiang Xu,[†] Hui M. Ge,[†] Jing Ma,[‡] Yong C. Song,[†] and Ren X. Tan*[,†]

[†]Institute of Functional Biomolecules, State Key Laboratory of Pharmaceutical Biotechnology, Nanjing University, Nanjing 210093, P. R. China

[‡]Institute of Theoretical and Computational Chemistry, Lab of Mesoscopic Chemistry, Nanjing University, Nanjing 210093, P. R. China

[∥]State Key Laboratory of Bioreactor Engineering, East China University of Science & Technology, Shanghai 200237, P. R. China

[§]College of Chemistry and Life Sciences, Zhejiang Normal University, Jinhua 321004, P. R. China

Supporting Information

ABSTRACT: Polyketides with unknown architectures are highly desired for the discovery of new drugs and agrochemicals. Here, the mantis-associated *Daldinia eschscholzii*, a fungus known to produce immunosuppressants dalesconols A and B, was found to simultaneously generate four novel skeletons capable of shaping the unusual chemistry of the fungal polyketides, of which seven were structurally unique and substantially immunosuppressive. In particular, the scaled-up fermentation of the microbe enabled the structural characterization of minor or "transitional" intermediate polyketides that allowed the reasonable recognition of the four biosynthetic pathways initiated by condensations of four, five, six and eight acetate units, respectively. Furthermore, the decarbonylation reaction of triketone, as in the case of daeschol A, was described for the first time, in addition to the structural correction of sporothrin C and nodulone. The work provided a set of novel immunosuppressive molecules that are of significance to drug discovery.

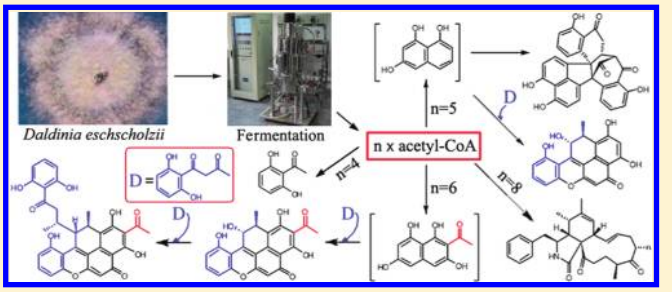

INTRODUCTION

Increasing numbers of organ transplantations and growing incidence of immune disorders such as arthritis and asthma leave patients in urgent need of new immunosuppressants. This matter is rendered even more pressing by the severe side effects noted with most existing immunosuppressive drugs, including cyclosporin A, glucocorticoids and cyclophosphamide.[1] Insect-microbe symbiosis is widespread, and targeting these organisms is an effective strategy for characterizing biologically active natural products with unique and unforeseeable architectures.[2] In light of our hypothesis that some insect-associated microorganisms may produce chemicals that kill or at least attenuate hosts' immune functions for their own habituation, we have discovered, from the broth of mantis-associated *Daldinia eschscholzii*, two novel immunosuppressive polyketides, dalesconols A and B (Scheme 1),[1b] which were synthesized by Snyder's group.[3]

Each organism on earth has to synthesize arrays of secondary metabolites (*viz.*, natural products), and their architecture differs through the editing of limited sets of building blocks through numerous pathways. Small molecule compounds produced in biological contexts may have unforeseeable structures and privileged scaffolds that can be important for the discovery of new drugs, herbicides and insecticides.[4] Furthermore, collections of natural products and natural-product-like compounds show higher success rates than typical synthetic chemical libraries.[5] Among versatile families of microbe- and plant-generated metabolites so far characterized, the polyketide is notable for its high success rate, which is close to 3‰ (20 marketed drugs out of some 7000 characterized polyketide structures).[4a] This fact, along with the difficulty and cost-ineffectiveness of the chemical construction of dalesconols A and B,[3] prompted us to scale up the growth of the fungus to identify other more potent immunosuppressive molecules with unforeseeable frameworks. To our surprise, a combination of column chromatography, gel filtration and HPLC purification of the extracts derived from the repeated fermentations of the title fungus gave a total of thirty-one polyketides including those representing four hitherto undescribed skeletons exemplified respectively by metabolites **5**, **15**, **22**, and **23**, and seven of the isolated compounds demonstrated immunosuppressive activity. The present cocharacterization of transitional and intermediate compounds generated mostly in trace amounts highlights the *D. eschscholzii* polyketide profile consisting of the four polyketide biosynthetic pathways illustrated in Schemes 1 and 3.

Received: December 6, 2010

   dx.doi.org/10.1021/ja110932p | *J. Am. Chem. Soc.* XXXX, XXX, 000–000

Scheme 1. ***Daldinia eschscholzii*** **Polyketides Starting from Four (Path I) and Five Acetyl-CoA (Path II) Condensations, the Latter of Which Affords Two Novel Carbon Skeletons Possessed by 5 and 15 (in solid rectangle), New Structures 6 and 10 (in dotted rectangle) and a Structural Revision of 16**

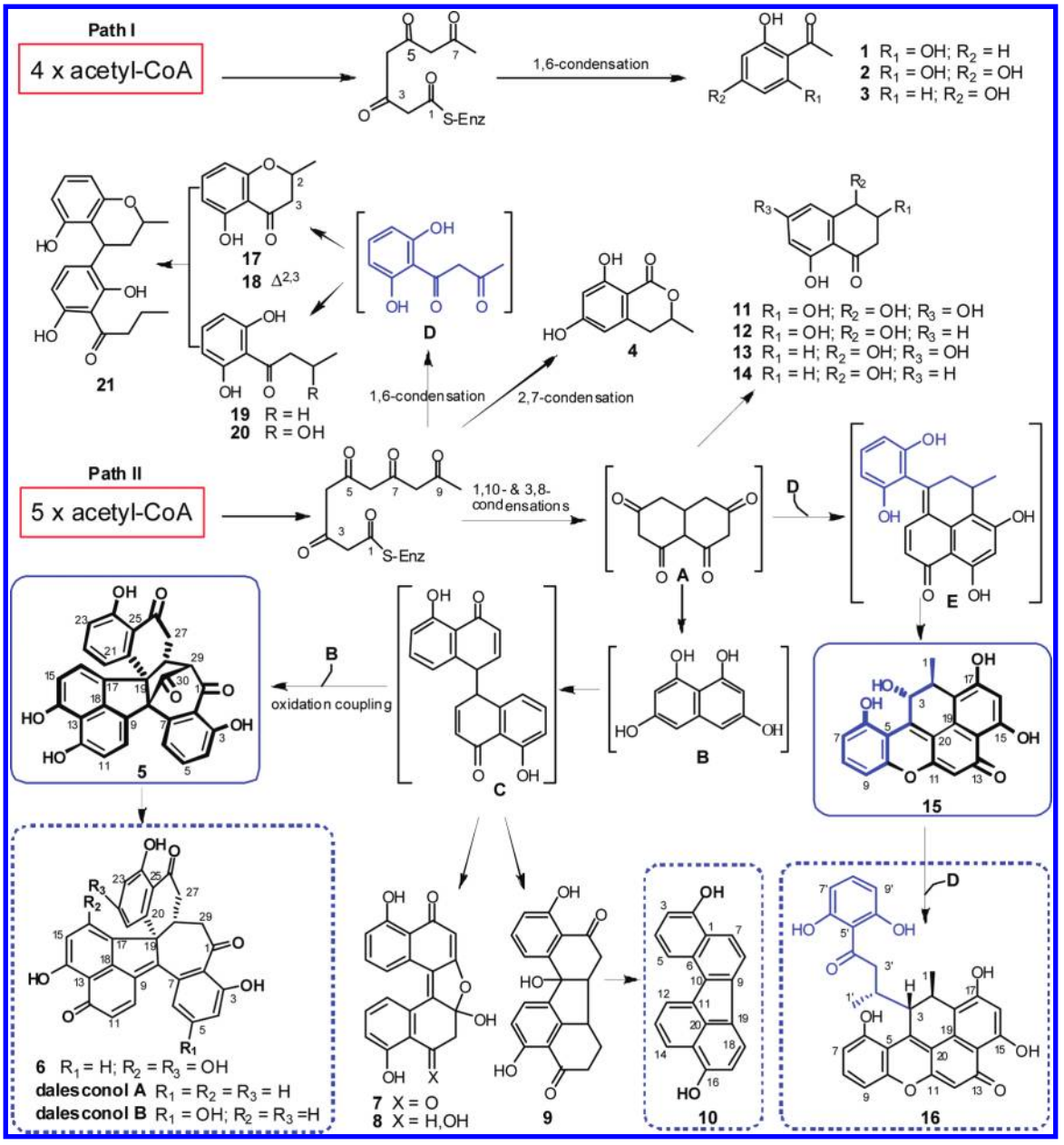

RESULTS AND DISCUSSION

The present scaled-up refermentations of the mantis-associated *D. eschscholzii* allows the characterization of the structures of more polyketides, some of which are unstable and/or only producible in minor or even trace quantities. The structure profile of these secondary metabolites made it reasonable to assume that the fungus grown in the given culture medium experienced at least the four polyketide biosynthetic pathways initiated by respective condensations of four, five, six and eight acetate units as highlighted by the isotope-labeled feeding experiments.[1b] In contrast to path **I**, which gave only three known acetophenones (**1**-**3**), pathway **II** assembled, in addition to dalesconols A and B,[1b] two more novel carbon skeletons, found respectively in daeschol A (**5**) and dalmanol A (**15**) together with two new polyketides, **6** and **10**.

Daeschol A (**5**), afforded as a gray powder, exhibited a quasi-molecular ion at m/z 491.1117 ($[M+H]^+$) in its high-resolution ESI mass spectrum (HR-ESI-MS), indicating its molecular formula to be $C_{30}H_{18}O_7$. In other words, it was dalesconol A with an extra C and O.[1b] This molecular formula was further substantiated by the ^1H and ^{13}C NMR spectra of **5**, which were strikingly different from those of dalesconol A. Specifically, the ^1H NMR spectrum of **5** gave altogether four phenolic, ten aromatic and two aliphatic methines and a set of methylene protons, and its ^{13}C NMR spectrum displayed a total of thirty

dx.doi.org/10.1021/ja110932p |*J. Am. Chem. Soc.* XXXX, XXX, 000–000

resonance lines that were grouped into three ketonic, fourteen quaternary, twelve methinic and one methylenic carbons as edited by the HMQC experiment and DEPT pulse sequences (Table 1). The unequivocal assignment of all ^{1}H and ^{13}C NMR spectral data of **5** was subsequently accommodated by the

Table 1. ^{1}H, ^{13}C and HMBC NMR Data for 5 in DMSO-d_6

Position	δ_C	δ_H (mult, J, Hz)	HMBC
1	201.8		
2	119.0		
3	162.2		
4	117.9	6.75 (br d, 8.0)	3, 6
5	138.0	7.36 (t, 8.0)	3, 7
6	118.8	6.97 (br d, 8.0)	4, 8
7	143.0		
8	79.7		
9	124.8		
10	127.3	7.43 (d, 7.6)	8, 12, 18
11	111.1	7.00 (d, 7.6)	9, 13
12	154.8		
13	113.7		
14	154.6		
15	111.8	6.79 (d, 7.6)	13, 17
16	123.4	7.41 (d, 7.6)	14, 18, 19
17	138.6		
18	141.7		
19	63.6		
20	145.6		
21	121.6	5.55 (br d, 8.0)	19, 23
22	137.8	6.91 (t, 8.0)	20, 24
23	116.3	6.45 (br d, 8.0)	21, 25
24	161.1		
25	118.1		
26	202.5		
27	37.3	α: 3.83 (dd, 17.6, 8.1)	19, 25, 29
		β: 3.04 (br d, 17.6)	19, 25, 29
28	41.9	3.56 (m)	17, 20, 26
29	70.6	3.87 (d, 5.8)	2, 8, 19, 27
30	201.1		
3−OH		11.38 (s)	3, 4
12−OH		10.40 (br s)	
14−OH		10.40 (br s)	
24−OH		12.09 (s)	23, 24

correlative interpretation of its COSY, NOESY, HMQC and HMBC spectra. In this molecule, the presence of 4,5-disubstituted naphthalene-1,8-diol moiety was required by two pairs of mutually coupling doublets (J = 7.6 Hz) at δ 7.43 and 7.00, and at δ 7.41 and 6.79. Moreover, a couple of 1,2,3-trisubstituted benzene nuclei were indicated by two groups of signals at δ 6.75 (br d, J = 8.0 Hz), 7.36 (t, J = 8.0 Hz) and 6.97 (br d, J = 8.0 Hz), and at δ 5.55 (br d, J = 8.0 Hz), 6.91 (t, J = 8.0 Hz) and 6.45 (br d, J = 8.0 Hz). The three aforementioned aromatic substructures were incorporated with three ketonic, two quaternary, two methinic and one methylenic nonaromatic carbons to form the most probable planar structure of **5** according to the HMBC correlations of the H-28 multiplet at δ 3.56 with C-17, C-20 and C-26, of the H-29 doublet (δ 3.87, J = 5.8 Hz) with C-2, C-8, C-19 and C-27, and of the broadened H-27 doublet (δ 3.04, J = 17.6 Hz) with C-19, C-25 and C-29. The proposed structure for **5** was further rationalized by the upfield movement of the H-21 resonance to δ 5.55 (d, J = 8.0 Hz) because of its positioning in the diamagnetic sphere of the naphthalene nucleus and by the two phenolic protons signifying as singlets at lower field at δ 11.38 (HO-3) and 12.09 (HO-24) owing to hydrogen bonds with the neighboring ketonic groups presumably via a six-membered ring. However, the HMBC spectrum of **5** is not informative enough due to the presence of the deprotonated cyclopentane core. Accordingly, the single-crystal X-ray crystallographic analysis was applied to confirm the novel carbon skeleton possessed by daeschol A (**5**) (Figure 1).[6] As encountered with dalesconols A and B,[1b] the crystal structure of **5** was demonstrated to be racemic by the space group $P2_1/n$ and the absence of any CD maximum. The subsequent chiral HPLC resolution of **5** afforded the anticipated enantiomers (+)-**5** and (−)-**5** (Figure 1), whose CD curves were completely reversed, although the ^{1}H and ^{13}C NMR data of the two enantiomers were identical. Starting from the relative stereochemistry evidenced from the single-crystal X-ray diffraction, the quantum chemical calculation on electric circular dichroism (ECD) was utilized to determine its absolute stereochemistry. As illustrated in Figure 2, the experimentally acquired CD spectrum for (−)-**5** matched the ECD curve computed for (8*R*,19*R*,28*R*,29*S*)-**5**. The first calculated positive Cotton effect at 210 nm could be assigned to the experimentally observed Cotton effect at 208 nm. The transitions from π-type to π^*-type molecular orbitals (MO), MO 123→136, contributed to this absorption band (Table S6 and Figure S77). The next two positive Cotton effects were located at 241 and 307 nm, which could be assigned to the experimentally discerned absorption bands at 255 and 310 nm, respectively. Among the excitations, those from *n*- (lone pair on carbonyl oxygen atoms) and π-type to π^*-type (C═C and C═O double bonds) orbital of phenyl

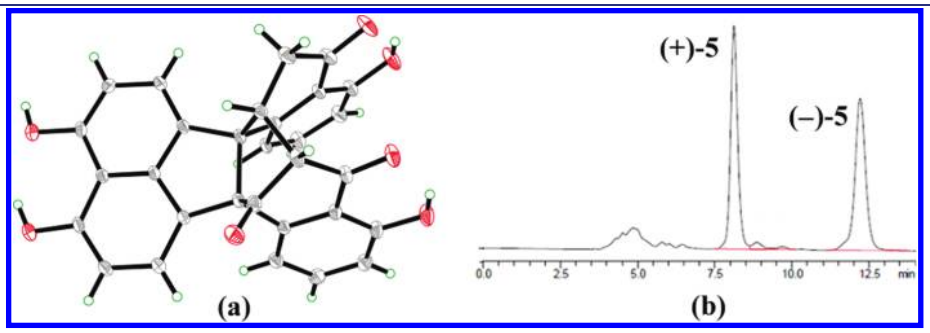

Figure 1. X-ray crystal structure (**a**, one H_2O molecule omitted for clarity) and chiral HPLC chromatogram (**b**) of **5**.

dx.doi.org/10.1021/ja110932p |*J. Am. Chem. Soc.* XXXX, XXX, 000–000

rings played a dominant role. In the experimental CD spectrum, the negative band observed at 235 nm, was also well reproduced by the calculations (at 237 nm). This Cotton effect was predominantly attributed to $\pi \rightarrow \pi^*$ excitation (MO 131→137). Another two broad negative bands around 277 and 340 nm were correlated with the calculated transition at 262 and 319 nm. Thus, we concluded the most probable absolute configuration of (−)-**5** to be *8R,19R,28R,29S* and its enantiomer *8S,19S,28S,29R*. Daeschol A (**5**) could be generated from trimerization of 1,8-naphthalenediol after experiencing keto−enol tautomerism, oxidation coupling and addition (Scheme 1).[10]

During its purification and analysis, daeschol A (**5**) was found to be quite unstable, and oxidized readily. Following stereochemical assignment, both enantiomers of **5** were shown be reductive and able to scavenge free radicals of 1,1-diphenyl-2-picryl-hydrazyl (DPPH) with the magnitude (IC_{50}: 25.6 and 33.3 μM for (+)-**5** and (−)-**5**, respectively) comparable to that (IC_{50}: 17.6 μM) of BHA (butyl hydroxy anisol) (Table S9). To our surprise, the main oxidated product of **5** was shown by TLC comparison to be dalesconol A, giving negligible antioxidative activity (IC_{50} > 200 μM) in the same assay. Furthermore, we also observed that daeschol A (**5**) was apt to gradually autoxidate and decarbonylate to form dalesconol A in solution where a single crystal was afforded. We therefore confirmed the conversion by treating **5** with 30% H_2O_2 to give dalesconol A an 81% yield at room temperature. This observation raised the possibility that the dalesconol A we discovered earlier could be an artifact of **5** that may autoxidate during fractionation.

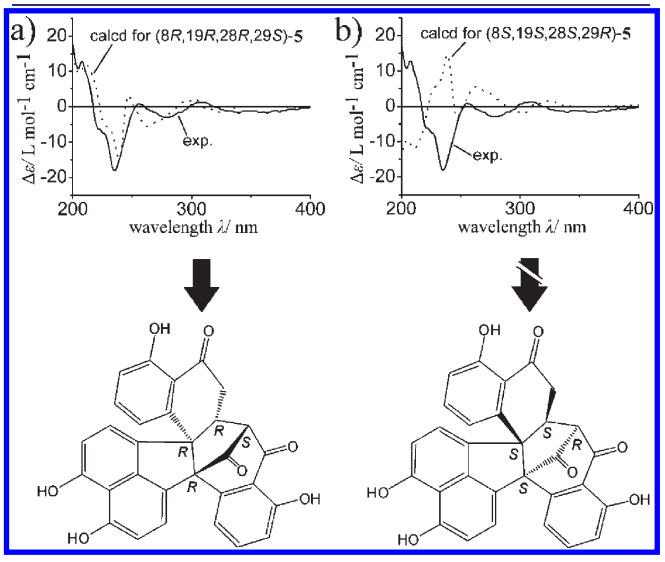

Figure 2. Attribution of the absolute configuration of (−)-daeschol A ((−)-**5**) as 8*R*,19*R*,28*R*,29*S* by comparing its experimental (solid curve) with the CD spectra computed for two options (dotted curve).

Accordingly, we checked for the copresence of **5** and dalesconol A by TLC and HPLC over a prolonged (22-day) fermentation. Surprisingly, daeschol A (**5**) was demonstrated to coexist constantly with dalesconol A (Figure S68), suggesting that **5** was most likely a biosynthetic intermediate of dalesconol A. Chemically, the decarbonylation of bridged heptadienone and dione was reported previously.[7] However, the decarbonylation of triketone encountered with daeschol A (**5**) seems hitherto unreported (Scheme 2). This reaction, undergoing in the fungal context, may be of importance in understanding and manipulating the biological and chemical pericyclic processes.[8]

Compound **6** was obtained as a red crystal with a molecular formula of $C_{29}H_{18}O_8$, as accommodated collectively by its HR-EI-MS and NMR spectral data. The ^1H and ^{13}C NMR spectra of **6** were very similar to those of dalesconol A.[1b] However, one 1,2,3,4-tetrasubstituted and one 1,2,3-trisubstituted benzene nuclei in the molecule of dalesconol A were simultaneously mono-oxidated in that of **6**. Subsequent 2D NMR (COSY, NOESY, HMQC and HMBC) and X-ray crystallographic (Figure 3)[6] analyses of **6** demonstrated that it was a 16,22-dihydroxylated derivative of dalesconol A. Again, the crystal space group indicated that it was a raceme. The chiral HPLC separation of **6** gave the corresponding enantiomers (+)-**6** and (−)-**6** (Figure 3), whose absolute configurations were found to be 19*S* and 28*R* and 19*R* and 28*S*, respectively, by comparing their CD spectra with those of (+)- and (−)-dalesconols A and B.[1b]

Compound **10**, having a molecular formula of $C_{20}H_{12}O_2$, showed its ^1H NMR spectrum to be very similar to that of benzo[*j*]fluoranthene (Table S3).[9] However, the 1D NMR spectrum of **10** gave two additional oxygenated olefinic carbon signals at δ_C 155.1 and 156.9 and two extra phenolic protons (δ_H 9.12 and 9.57, exchangeable with D_2O). These observations indicated that its structure was 2,16-dihydroxybenzo-[*j*]fluoranthene. These findings were supported by the long-range correlations of C-2 to H-3, H-4 and H-7, and of C-16 to H-14 and H-18 in its HMBC spectrum.

Dalmanol A (**15**), isolated as a red needle, gave a $[M\text{-}H]^-$ ion peak at *m/z* 349.0720 in its negative-mode HR-ESI-MS, indicating its molecular formula to be $C_{20}H_{14}O_6$. This was in accordance with the fourteen-hydrogen integration and twenty-carbon resonance lines in its ^1H and ^{13}C NMR spectra (Table 2). In correlation with DEPT experiments, the ^{13}C NMR spectrum displayed a total of twenty signals that were grouped into one methyl, two sp^3- and five sp^2-hybridized methinic, eleven sp^2-hybridized quaternary and a ketonic (δ 187.5) carbons. The ^{13}C NMR resonance profile demonstrated the presence of 1,2,3-tri- and 1,2,3,4,5-penta-substituted benzene rings if correlated with the one-proton NMR signals at δ 6.87 (br d, 8.2), 7.47 (t, 8.2), 6.96 (br d, 8.2), and 6.47 (s). Furthermore, a 1,2-disubstituted propanol scaffold was required by the signals at δ 0.95 (3H, d, 7.0), 3.46 (1H, br q, 7.0), and 5.89 (1H, br s). With the

Scheme 2. Autooxidation of 5 into Dalesconol A

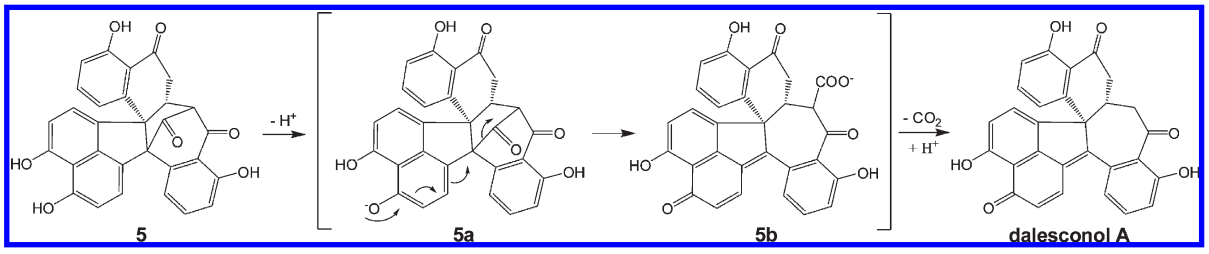

dx.doi.org/10.1021/ja110932p |J. Am. Chem. Soc. XXXX, XXX, 000–000

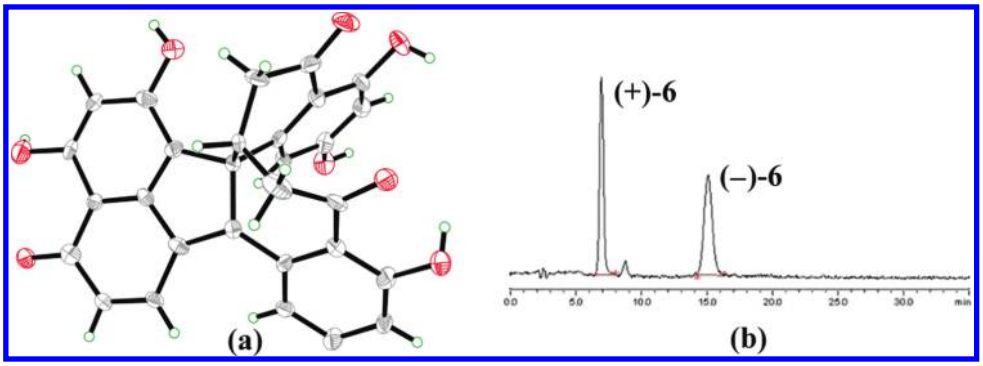

Figure 3. X-ray crystal structure (**a**, solvent molecules omitted for clarity) and chiral HPLC chromatogram (**b**) of **6**.

Scheme 3. ***Daldinia eschscholzii*** **Polyketides Starting from Six- (path III) and Eight-acetyl-CoA (path IV) Condensations, Generating Two Novel Carbon Skeletons Possessed by 22 and 23 (in solid rectangle), New Structures 27 and 29 (in dotted rectangle) and Structural Revision of 28**

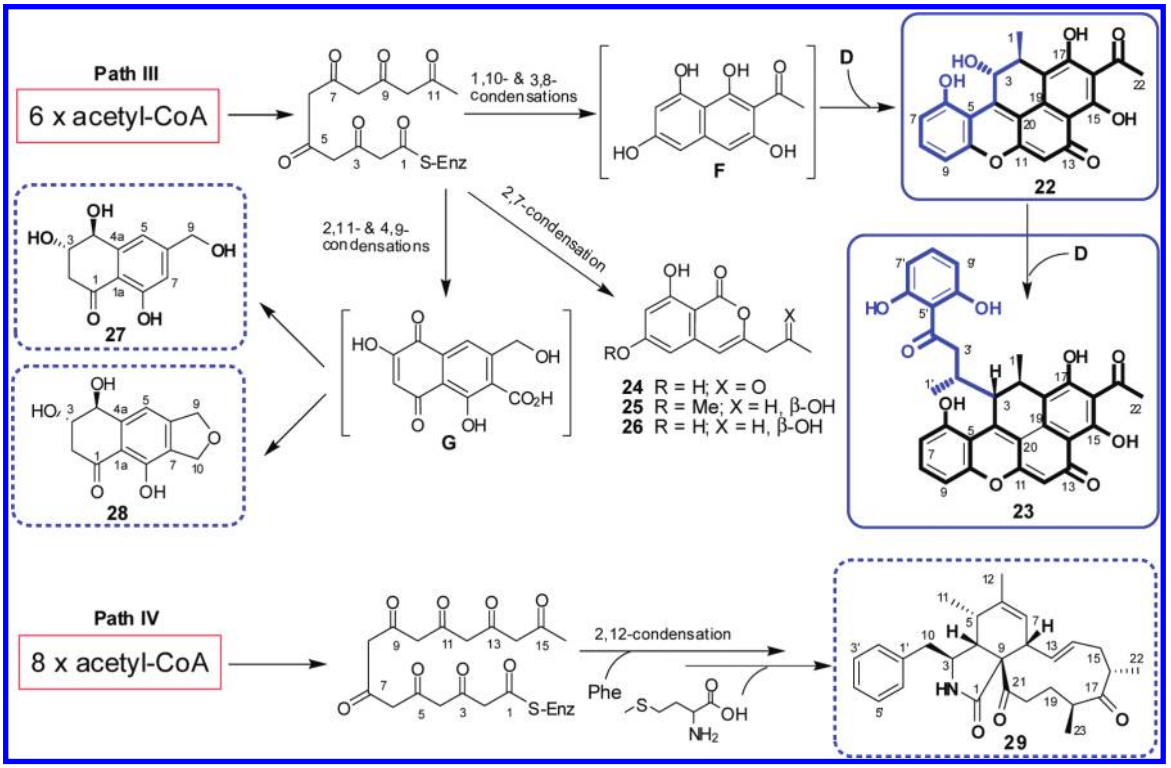

unsaturation indices of the molecular formula in mind, these three substructures were combined into the most probable molecule by editing the rest five (one methinic and four quaternary) sp^2-hybridized carbons according to the key HMBC correlations of H-2 (δ 3.46) with C-4, C-17 and C-19, of H-3 (δ 5.89) with C-1, C-5 and C-18, and of the H-12 singlet at δ 6.08 with C-14 and C-20. Implied by the proposed structure of **15**, the downfield movement of HO-15 to δ 13.95 was allowed by its stable hydrogen-bonding with 13-carbonyl group. The given relative stereochemistry of **15**, determined by the NOESY spectrum, was finally confirmed by X-ray analysis (Figure 4).[6] Again, the crystal space group *P*-1 indicated that it was a raceme that was separated by chiral HPLC into the enantiomers (+)-**15** and (−)-**15** (Figure 4), both possessing a reverse CD curve and optical rotations but identical ^{1}H and ^{13}C NMR spectra. The absolute stereochemistry of (−)-enantiomer (−)-**15** was determined by quantum chemical CD calculations. Displayed in Figure 5 were the calculated ECD spectra of the two enantiomers, (*2R,3S*)-**15** and (*2S,3R*)-**15**, the former matching the experimentally acquired CD curve of (-)-**15**. The first three negative Cotton effects were located at 340, 244, and 223 nm, which could be assigned to the experimentally observed absorption bands at 348, 250, and 219 nm, respectively. Among these excitations, those from the π-type to π^*-type (C=C double bonds in phenyl rings) orbital of phenyl rings played a dominant role. The last calculated negative Cotton effect at 464 nm could be assigned to the experimentally discerned Cotton effect at 461 nm. The transition from a π-type (MO 91, HOMO) to a π^*-type (MO 92, LUMO) molecular orbital contributed to this broad absorption band (Table S7 and Figure S78). In the

dx.doi.org/10.1021/ja110932p |*J. Am. Chem. Soc.* XXXX, XXX, 000–000

Table 2. ^{1}H, ^{13}C and HMBC NMR Data for 15 and 22 in DMSO-d_6

	15			22		
position	δ_C	δ_H (mult, J, Hz)	HMBC	δ_C	δ_H (mult, J, Hz)	HMBC
1	17.4	0.95 (d, 7.0)	3, 18	16.3	0.98 (d, 7.3)	2, 3, 18
2	33.0	3.46 (br q, 7.0)	4, 17, 19	32.2	3.52 (br dq, 1.3, 7.3)	1, 3, 4, 17, 18, 19
3	66.3	5.89 (br s)	1, 5, 18	65.7	5.97 (br s)	1, 4, 5, 18, 20
4	142.9			146.9		
5	109.5			108.8[a]		
6	158.5			158.2		
7	112.7	6.87 (br d, 8.2)	5, 9	112.5	6.91 (br d, 8.2)	5, 6, 9
8	133.6	7.47 (t, 8.2)	6, 10	134.8	7.57 (t, 8.2)	6, 10
9	107.7	6.96 (br d, 8.2)	5, 7	107.5	7.02 (br d, 8.2)	5, 7, 10
10	154.0			154.0		
11	160.0			160.3		
12	101.3	6.08 (s)	11, 14, 20	100.6	6.22 (s)	11, 14, 20
13	187.5			187.1		
14	107.2			106.4		
15	161.5			166.1		
16	102.8	6.47 (s)	14, 18	109.0[a]		
17	159.8			163.6		
18	115.8			114.8		
19	127.5			131.9		
20	115.1			113.9		
21				205.2		
22				33.3	2.77 (s)	16, 21
3-OH		5.30 (br s)			5.50 (br s)	
6−OH		11.10 (s)	5, 6		11.39 (s)	5
15−OH		13.95 (s)	14, 15, 16		16.98 (s)	14, 15, 16
17−OH		10.49 (s)	16, 17, 18		14.18 (s)	16, 17, 18

[a] Interchangeable assignments.

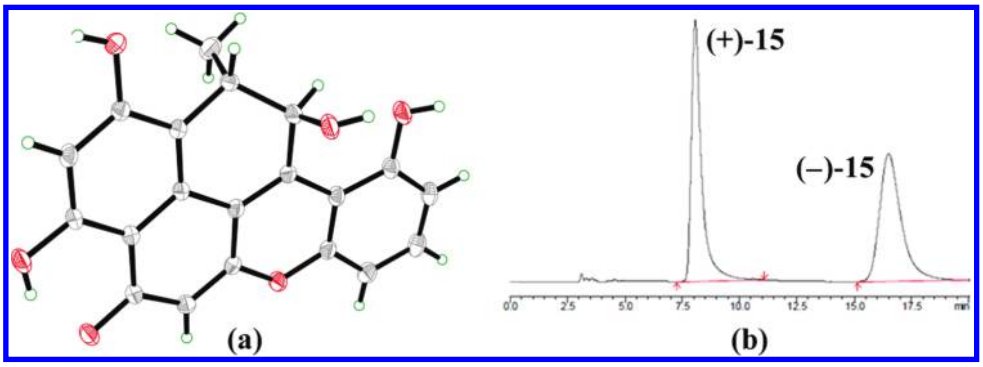

Figure 4. X-ray crystal structure (**a**, H_2O molecule omitted for clarity) and chiral HPLC chromatogram (**b**) of **15**.

experimental CD spectrum, a positive band at 276 nm with a shoulder (near 320 nm) was also well reproduced by the calculation (at 304 nm). It arose predominantly from $\pi \rightarrow \pi^*$ excitation (from MOs 91 to 93). Another broad positive band near 390 nm was correlated with the calculated transition at 385 nm, representing mainly the excitations from MOs 89 to 92, and from MOs 90 to 92. Thus, the absolute stereochemistry of (−)-enantiomer ((−)-**15**) was found to be 2*R*,3*S*, and its enantiomer ((+)-**15**) had to bear 2*S*,3*R*-configurations.

Compound **16** possessed a molecular formula of $C_{30}H_{24}O_8$, corresponding to the $[M+Na]^+$ peak at m/z 535.1369 in its HR-ESI-MS. If exempting the proton and carbon-13 signals due to a 3-substituted 1-(2,6-dihydroxyphenyl)butan-1-one moiety, the ^{1}H and ^{13}C NMR spectra of **16** (Table 3) were close in part to those of **15**, despite the striking difference in resonances arising from the 1,1,2-trisubstituted propane residue. This observation could only be explained by assuming the attachment to C-3 of the 3-substituted 1-(2,6-dihydroxyphenyl)butan-1-one residue. This assumption was subsequently confirmed by a correlative interpretation of its 2D NMR spectra, which allowed the exact assignment of its relative stereochemistry as well as all ^{1}H and ^{13}C NMR signals. To our surprise, the ^{1}H and ^{13}C NMR data were almost identical to

dx.doi.org/10.1021/ja110932p |J. Am. Chem. Soc. XXXX, XXX, 000–000

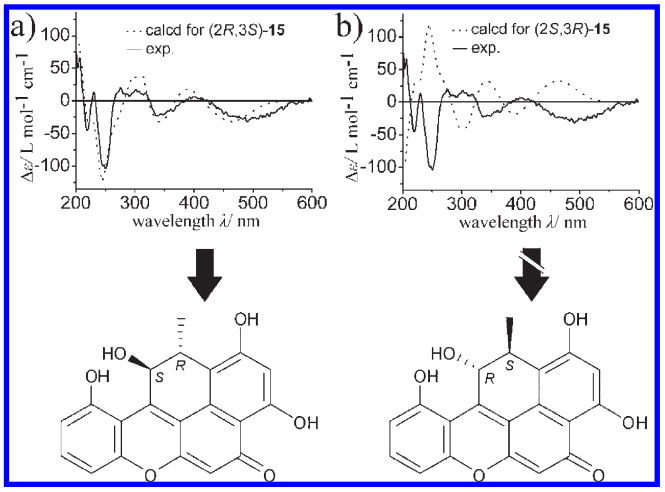

Figure 5. Attribution of the absolute configuration of (+)- and (−)-dalmanol A (**15**) as 2*S*,3*R* and 2*R*,3*S* by comparing the experimental (solid curve) and calculated (dotted curve) CD spectra.

those of the sporothrin C that was characterized as a metabolite of *Sporothrix* sp. (#4335).[10] However, we clearly detected the key HMBC correlations of 10′−OH to C-5′ and C-9′, and of 17-OH to C-18, suggesting that the structure of sporothrin C should be revised as **16**. The chiral HPLC separation of **16** gave the corresponding enantiomers (+)-**16** and (−)-**16** (Figure S69), which were shown to possess 2*R*,3*R*,2′*R*- and 2*S*,3*S*,2′*S*- configurations, respectively, by comparison of their CD spectra to those of (+)-**23** and (−)-**23** (Figures S74 and S76).

Also chemically promising is pathway **III**, which constructs two more novel carbon skeletons, represented by acetodalmanols A (**22**) and B (**23**), in addition to a new compound (**27**) (Scheme 3). The HR-ESI-MS of compound **22** indicated that it possessed a molecular formula of $C_{22}H_{16}O_7$, one C_2H_2O more than that of **15**. The subsequent comparison of its ^{1}H and ^{13}C NMR spectra to those of dalmanol A (**15**) (Table 2) highlighted that it carried a benzene-bonded acetyl group affording NMR signals at δ_H 2.77 and δ_C 33.3 and 205.2. Furthermore, the singlet of H-16 at δ_H 6.47, discernible in the ^{1}H NMR of **15**, was missing in that of **22**. Along with its HMBC correlations of H-22 to C-16, these dissimilarities indicated that **22** was a 16-acetyl derivative of **15**. To check the enantiomeric purity, compound **22** was subjected to chiral HPLC separation to give (+)-**22** and (−)-**22** in a proportion of 95.6:4.4 (Figure S70). The CD spectrum of (+)-enantiomer ((+)-**22**) exhibited Cotton effects similar to those of (+)-**15**, suggesting that (+)-**22** carried as well a 2*S*,3*R*-configuration, and (−)-**22** had to be 2*R*,3*S*-structured (Figures S73 and S75).

Acetodalmanol B (**23**) was deduced from its HR-ESI-MS to have a molecular formula of $C_{32}H_{26}O_9$, one C_2H_2O more than that of **16**. Furthermore, the ^{1}H and ^{13}C NMR data of **23** resembled those of **16** except for signals at δ_H 2.71 and δ_C 33.1 and 204.8, which could be readily ascribed to a benzene-bonded acetyl group (Table 3). This observation, along with the HMBC correlations of H-22 to C-16, highlighted that compound **23** was a 16-deacetyl derivative of **16**. Detailed analysis of its 2D NMR data (COSY, ROESY, HMQC and HMBC) was in full agreement with the proposed structure. To achieve enantiomer resolution, compound **23** was separated by chiral HPLC into (+)-**23** and (−)-**23** (Figure S71). The absolute configuration of (+)-**23** was determined by scrutinizing its computational and experimental CD curves (Figure 6). The calculated ECD curve

Table 3. ^{1}H and ^{13}C NMR Data for 16 and 23 in DMSO-d_6

	16		23	
position	δ_C	δ_H (mult, *J*, Hz)	δ_C	δ_H (mult, *J*, Hz)
1	21.2	1.03 (d, 7.0)	21.2	1.04 (d, 7.0)
2	24.2	3.48 (br q, 7.0)	23.0	3.54 (br q, 7.0)
3	45.1	4.35 (br d, 3.7)	45.5	4.32 (br d, 2.5)
4	146.8		152.0	
5	109.8		109.8	
6	157.0		157.7	
7	112.0	6.86 (br d, 8.2)	112.3	6.93 (br d, 8.2)
8	132.9	7.47 (t, 8.2)	134.4	7.57 (t, 8.2)
9	107.6	6.96 (br d, 8.2)	107.7	7.02 (br d, 8.2)
10	153.2		153.6	
11	158.4		158.8	
12	99.9	5.94 (s)	99.6	5.99 (s)
13	186.8		186.6	
14	107.4		106.2	
15	160.6		165.9	
16	102.5	6.42 (s)	108.5	
17	158.2		162.2	
18	115.4		114.3	
19	127.6		132.3	
20	115.2		113.9	
21			204.8	
22			33.1	2.71 (s)
6−OH		11.15 (s)		11.51 (s)
15−OH		13.93 (s)		16.90 (s)
17−OH		10.29 (s)		14.25 (s)
1′	18.4	1.01 (d, 6.8)	19.6	1.16 (d, 7.0)
2′	33.5	2.59 (m)	33.7	2.78 (dq, 7.0, 2.5)
3′	46.3	α: 2.51 (dd, 16.8, 9.8)	45.9	α: 2.38 (dd, 17.6, 6.1)
		β: 2.85 (dd, 16.8, 3.6)		*β*: 3.18 (dd, 17.6, 7.5)
4′	206.3		205.7	
5′	111.3		110.0	
6′, 10′	160.2		160.8	
7′, 9′	106.8	6.20 (d, 8.2)	106.7	6.12 (d, 8.2)
8′	134.7	7.06 (t, 8.2)	135.2	7.08 (t, 8.2)
6′,10′−OH		11.00 (s)		11.15 (s)

for (2*R*,3*R*,2′*R*)-**23** matched the experimentally measured CD spectrum of (+)-**23**. The calculated positive Cotton effects at 289, 403, and 498 nm could be assigned to the bands centered at 293, 373, and 497 nm in the experimental CD spectrum, respectively. The electronic excitations from lone pair orbitals of oxygen and filled C=C molecular orbitals (designated as n_O and $\pi_{C=C}$ MO, respectively) to π^*-type C=C and C=O orbitals ($\pi^*_{C=C}$ and $\pi^*_{C=O}$), MO 143→146, MO 143→148, and MO 145→146, contributed dominantly to these absorption bands as shown in Table S8 and Figure S79. The electronic transitions from $\pi_{C=C}$ to $\pi^*_{C=C}$ orbitals (MO 135→146) played a key role in the negative rotatory strengths at 253 nm. It associates with the experimental Cotton effect at 274 nm. Accordingly, the absolute configuration of (+)-**23** was determined as 2*R*,3*R*,2′*R*, and the 2*S*,3*S*,2′*S*-configurations had to be assigned for (−)-**23**.

Compound **27** ($C_{11}H_{12}O_5$) gave ^{1}H and ^{13}C NMR spectra that were very similar to those of **12**, if neglecting the signals ascribable to

dx.doi.org/10.1021/ja110932p |*J. Am. Chem. Soc.* XXXX, XXX, 000–000

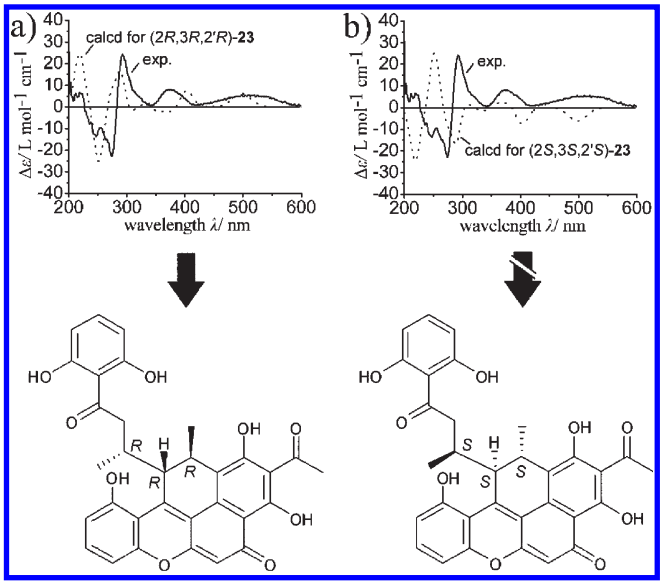

Figure 6. Attribution of the absolute configuration of (+)- and (−)-acetodalmanol B (**23**) as 2*R*,3*R*,2′*R* and 2*S*,3*S*,2′*S* by comparison of the experimental (solid curve) and calculated (dotted curve) CD spectra.

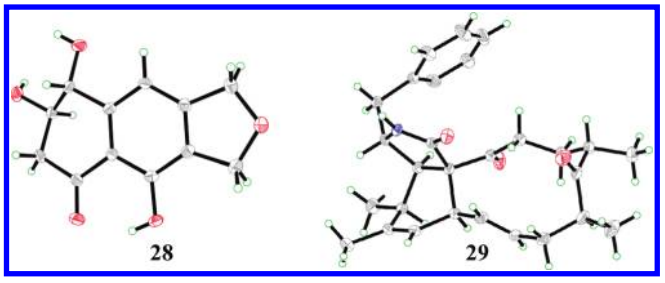

Figure 7. X-ray crystal structures of **28** and **29**.

oxymethylene (δ_H 4.65 and δ_C 64.3) and one of the hydroxyl groups (δ_{OH} 4.47, exchangeable with D_2O) (Table S4).[11] This observation, along with a set of 2D NMR experiments (COSY, NOESY, HMQC and HMBC), showed that it was 3,4,8-trihydroxy-6-(hydroxymethyl)-3,4-dihydronaphthalen-1(2H)-one, and the coupling constant and NOESY spectrum indicated that compound **27** shared the same relative configuration with that of nodulone (**28**, see below).

Compound **28** ($C_{12}H_{12}O_5$), obtained as a colorless crystal, was identified as nodulone by comparing its MS, ^1H and ^{13}C NMR spectral data with those in literature (Table S4).[12] Moreover, its relative stereochemistry was reassigned by our X-ray crystallographic analysis (Figure 7).[6]

Pathway **IV** assembled a new cytochalasin derivative **29**, most likely following the steps summarized recently.[13] Aided by 2D NMR experiments (COSY, ROESY, HMQC and HMBC), a correlative interpretation of the HR-ESI-MS and ^1H and ^{13}C NMR spectra of **29** suggested that it was a 17-keto-19(20)-hydroderivative of cytochalasin 11 (Table S5).[14] The proposal was confirmed by single-crystal X-ray analysis leading to the assignment of its relative configuration (Figure 7).[6] We have named compound **29** neocytochalasin.

In addition to recognizing both enantiomers of daeschol A (**5**) as a potent free radical scavengers, our immunosuppressive assay indicated that compounds (+)-**5**, **10**, (+)-**15**, (−)-**15**, **22**, (+)-**23** and (−)-**23** were substantially active with corresponding IC_{50} values 5.96, 0.025, 1.72, 5.56, 5.00, 0.87, and 2.14 μg/mL, respectively, and the IC_{50} data of cyclosporin A (coassayed as a positive reference) was 0.06 μg/mL. Furthermore, compounds **10**, (+)-**23** and (−)-**23** were also cytotoxic with IC_{50} values of 0.22, 14.34, and 10.04 μg/mL, whereas other polyketides were trivially active (IC_{50} > 80 μg/mL) (Table 4). These data also showed that the difference in bioactivities between pairs of enantiomers depends on the structural framework to some extent.

Table 4. *In vitro* Inhibitory Effects of *D. eschscholzii* Polyketides on ConA-induced Proliferation of Mouse Spleen Cells

	IC_{50} (μg mL^{-1})[a]		
Compounds	ConA-induced	Cytotoxicity	SI[c]
5	>10.00	>80.00	
(+)-**5**	5.96 ± 0.06	>80.00	>13.4
(−)-**5**	>10.00	>80.00	
6	>10.00	N/T[d]	
10	0.025 ± 0.002	0.22 ± 0.03	8.8
15	>10.00	>80.00	
(+)-**15**	1.72 ± 0.10	>80.00	>46.5
(−)-**15**	5.56 ± 0.17	>80.00	>14.4
16	>10.00	N/T[d]	
22	5.00 ± 0.55	>80.00	>16.0
23	2.62 ± 0.15	12.84 ± 0.36	4.9
(+)-**23**	0.87 ± 0.05	14.34 ± 0.42	16.5
(−)-**23**	2.14 ± 0.15	10.04 ± 0.71	4.7
28	>10.00	21.27 ± 1.11	
29	>10.00	N/T[d]	
cyclosporin A[b]	0.06 ± 0.002	11.20 ± 0.68	187.0

[a] The IC_{50} values are expressed as mean ± standard error of three determinations. [b] Co-assayed as a positive control. [c] Selectivity index [SI] determined as the ratio of the IC_{50} values on resting mouse spleen cells viability (cytotoxicity) to the IC_{50} on the activated proliferation of mouse spleen cells. [d] Not tested.

In summary, four novel carbon skeletons, illustrated by daeschol A (**5**), dalmanol A (**15**) and acetodalmanols A (**22**) and B (**23**), were characterized from the regrown biomass of the title mantis-associated fungus, highlighting that the insect-derived microbes could be a fruitful source of novel bioactive secondary metabolites. The natural products cocharacterized in the present work suggest collectively that the four polyketide biosynthetic pathways the title fungus can run simultaneously. Moreover, the autoxidation of daeschol A to dalesconol A underpins a hitherto unreported decarbonylation reaction of some organic compounds with suitably structured triketone moiety. In conjunction with antioxidative and immunosuppressive assays, the investigation has identified from the thirty-one polyketides, among which a set of the novel free radical scavengers and immunosuppressors with novel structures may be valuable for the discovery of relevant drugs.

EXPERIMENTAL SECTION

Strain and cultivation. The procedures of isolation and identification of the fungal strain used in this experiment were described in an earlier study.[1b] The fresh mycelium was inoculated into 1 L flask preloaded with 400 mL of ME medium (consisting of 20 g malt extract, 20 g sucrose and 1 g peptone in 1 L of distilled water) followed by a four-

dx.doi.org/10.1021/ja110932p |J. Am. Chem. Soc. XXXX, XXX, 000–000

day culture at 200 rpm/min and 28 °C. The whole liquid (10 × 400 mL) collected from the flask was inoculated onto a 50-L seed tank containing 38 L of sterilized ME medium (antifoam 0.1‰, aeration rate 2000 NL/h, 150 rpm/min). After a subsequent fermentation at 28 °C for 24 h, the afforded liquid was transferred as seed into the 500 L fermentator preloaded with 300 L of sterilized ME medium prior to cultivation at 28 °C for 4 days (antifoam 0.1‰, aeration rate 6000 NL/h, 150 rpm/min). The fractionation procedure is detailed in Supporting Information.

Computational details. For these systems, we first carried out full geometry optimization in CH_3OH by density functional theory (DFT) at the B3LYP/6-31G(d) level. The solvation effects on the electronic structures of the systems studied were evaluated by quantum chemistry methods through the polarized continuum model (PCM, dielectric constant $\varepsilon = 32.63$). Then, the corresponding excited-state calculations were performed at ground-state optimized geometries. Time-dependent DFT in combination with PCM (TD-DFT/PCM) with the same basis set was carried out to calculate the spin-allowed excitation energy and rotatory strength of the lowest 120 excited states. The final ECD spectra were obtained according to the following equations:[15]

$$\Delta\varepsilon(\lambda) = \sum_n \Delta\varepsilon_n \exp\left[-\left(\frac{\lambda-\lambda_n}{\Delta\lambda_n}\right)^2\right] \quad (1)$$

$$\Delta\varepsilon_n = \frac{\lambda_n R_n}{22.94\sqrt{\pi}\Delta\lambda_n} \times 10^{40} \quad (2)$$

Where $\Delta\varepsilon_n$ is the peak intensity given in L mol^{-1} cm^{-1}, R_n is the rotatory strength in unit of 10^{-40} cgs, λ_n is the wavelength of the nth transition and $\Delta\lambda_n$ is the half-width at $1/e$ of peak maximum. Here we used half-width $\Delta\lambda_n = \lambda_n^2\Delta\tilde{\nu}$ with $\Delta\tilde{\nu} = 2000cm^{-1}$. All calculations were performed using the Gaussian03 program.[16]

Oxidation of daeschol A (5). To a solution of **5** (5.0 mg, 1.02 × 10^{-2} mmol) in 5 mL of acetone was added 5 mg (4.41 × 10^{-2} mmol) of 30% H_2O_2. The mixture was stirred for 4.5 h at room temperature and then concentrated *in vacuo*. The residue was purified by Sephadex LH-20 to provide dalesconol A (3.8 mg).

Tracing daeschol A (5) and dalesconol A in the culture. The fresh mycelium of *D. Eschscholzii* was inoculated into a 250 mL flask containing 150 mL of ME medium. After a two-day incubation at 28 °C with an agitation of 150 rpm, 20 mL of culture liquid was transferred as seed into each 250 mL flask containing 150 mL of ME medium. Cultivation was kept at 30 °C with an agitation of 130 rpm. Day by day, a part of the culture liquid was taken and extracted immediately with EtOAc, and the extract was checked for the presence of daeschol A (**5**) and dalesconol A by TLC and HPLC (Figure S68). To further confirm their copresence in the culture, material derived from the tests was purified by chromatography over a silica gel column ($CHCl_3$/MeOH, gradient 100:0→25:8), leading to the isolation of **5** and dalesconol A.

Biological testing. The *in vitro* immunosuppressive activity and cytotoxicity were evaluated by T-cell viability and MTT assays as described in our previous papers.[1b,17] The scavenging effects of samples for DPPH radical were monitored according to the method detailed in previous reports.[18]

Daeschol A (5). Gray crystals, mp 288−290 °C; UV (MeOH): λ_{max} nm (log ε)=465 (0.90), 342.5 (1.60), 210.5 (2.17); IR (KBr) ν_{max}: 3564.2, 3406.8, 2960.4, 1770.4, 1638.8, 1608.0, 1572.2, 1448.2, 1399.5, 1336.5, 1251.3, 1227.5, 1194.9, 1155.7, 814.8, 748.0, 713.0 cm^{-1}; HR-ESI-MS: m/z 491.1117 $[M+H]^+$, calcd for $C_{30}H_{19}O_7$, 491.1131; ^{1}H (500 MHz) and ^{13}C NMR (125 MHz) in DMSO-d_6 see Table 1. (−)-**5**: $[\alpha]^{20}_D$= −91.0°(c = 0.01 in MeOH); CD (MeOH): λ_{max} nm ($\Delta\varepsilon$)=207.8 (+20.69), 235.3 (−29.12), 255.3 (+1.31), 277.1 (−4.77), 310.0 (+1.97), 339.7 (−2.82). (+)-**5**: $[\alpha]^{20}_D$= +90.4° (c = 0.01 in MeOH); CD (MeCN): λ_{max} nm ($\Delta\varepsilon$)=205.5 (−21.43), 234.1 (+28.25), 256.5 (−0.15), 283.8 (+5.85), 309.6 (−0.51), 341.6 (+3.28).

Dalesconol C (6). Red crystals, mp 306−308 °C; UV (MeOH): λ_{max} nm (logε)=384.5 (2.23), 327 (2.43), 281 (2.46), 237.5 (2.71), 204.5 (2.92); EI-MS m/z 494 $[M]^+$, HR-EI-MS: m/z calcd for $C_{29}H_{18}O_8$ $[M]^+$: 494.1002; found: 494.1031. ^{1}H (500 MHz) and ^{13}C NMR (75 MHz) in acetone-d_6 see Table S2.

2,16-Dihydroxyl-benzo[*j*]fluoranthene (10). Yellow powder, m.p.253−255 °C; UV (MeOH): λ_{max} nm (logε): 399 (1.41), 379 (1.38), 334 (1.88), 243 (1.99); IR (KBr) ν_{max}: 3417.8, 1611.8, 1583.5, 1426.1, 1246.6, 807.9, 747.5 cm^{-1}; ^{1}H (300 MHz) and ^{13}C NMR (75 MHz) in acetone-d_6 see Table S3. HR-ESI-MS: m/z 307.0726 $[M+Na]^+$, calculated for $C_{20}H_{12}O_2Na^+$ 307.0730.

Dalmanol A (15). Red crystals, mp 124−126 °C; UV (MeOH): λ_{max} nm (logε)=489 (2.18), 375 (2.21), 277 (2.28), 254 (2.57), 229 (2.84), 203 (2.97); HR-ESI-MS: m/z 349.0720 $[M-H]^-$, calcd for $C_{20}H_{13}O_6$, 349.0718; ^{1}H (500 MHz) and ^{13}C NMR (125 MHz) in DMSO-d_6 see Table 2. (−)-**15**: $[\alpha]^{20}_D$= −1389°(c = 0.02 in MeOH); CD (MeOH): λ_{max} nm ($\Delta\varepsilon$)=219 (−87.08), 250.5 (−199.15), 275.9 (+39.32), 317.3 (+22.24), 348.5 (−41.19), 392.6 (+11.30), 461.0 (−45.96). (+)-**15**: $[\alpha]^{20}_D$= +1386° (c = 0.02 in MeOH); CD (MeOH): λ_{max} nm ($\Delta\varepsilon$)=219.3 (+52.03), 251.2 (+152.05), 274.4 (−20.88), 315.9 (−10.39), 350.5 (+40.32), 409 (−0.12), 462.1 (+41.89).

Dalmanol B (16). Red crystals, mp 305−307 °C; UV (MeOH): λ_{max} nm (logε): 478 (2.57), 325 (2.80), 310 (2.78); IR (KBr) ν_{max} (cm^{-1}): 3410.2, 2927.6, 1725.6, 1601.6, 1460.5, 1228.1, 1178.6, 891.3; ^{1}H (500 MHz) and ^{13}C NMR (125 MHz) in DMSO-d_6 see Table 3. HR-ESI-MS: m/z 535.1369 $[M+Na]^+$, calculated for $C_{30}H_{24}O_8Na^+$ 535.1363. (−)-**16**: $[\alpha]^{20}_D$= −415° (c = 0.01 in MeOH); CD (MeOH): λ_{max} nm ($\Delta\varepsilon$)=271.3 (+14.14), 290.4 (−10.24), 302.4 (−0.27), 335.7 (−5.43), 346.3 (−1.45), 371.2 (−5.55), 427.2 (−0.35), 500.0 (−8.30). (+)-**16**: $[\alpha]^{20}_D$= +420° (c = 0.01 in MeOH); CD (MeOH): λ_{max} nm ($\Delta\varepsilon$)=270.1 (−5.10), 293.5 (+9.75), 304.3 (+1.36), 336.9 (+6.48), 344.8 (+2.91), 374.6 (+6.90), 422.0 (+0.67), 496.2 (+9.44).

Acetodalmanol A (22). Red crystals, m.p.239−241 °C; UV (MeOH): λ_{max} nm (log ε): 506.0 (1.94), 361.0 (2.06), 286.0 (2.28), 242.0 (2.21), 216.0 (2.31); IR (KBr) ν_{max}: 3456.6, 2648.7, 1632.6, 1604.3, 1556.7, 1433.9, 1220.7, 1177.9, 1136.6, 1028.5, 874.0, 797.0, 773.8 cm^{-1}; ^{1}H (500 MHz) and ^{13}C NMR (125 MHz) in DMSO-d_6 see Table 2. HR-ESI-MS: m/z 415.0822 $[M+Na]^+$, calculated for $C_{22}H_{16}O_7Na^+$ 415.0788. (−)-**22**: $[\alpha]^{20}_D$ = −655° (c = 0.01 in MeOH); CD (MeOH): λ_{max} nm ($\Delta\varepsilon$) = 263.1 (−28.53), 308.1 (−1.35), 319.6 (−5.30), 347.6 (+3.86), 393.6 (−6.00), 411.9 (−2.56), 510.6 (−15.77). (+)-**22**: $[\alpha]^{20}_D$ = +658° (c = 0.01 in MeOH); CD (MeOH): λ_{max} nm ($\Delta\varepsilon$)= 262.7 (+28.84), 303.0 (+1.21), 319.6 (+5.35), 348.3 (−4.09), 394.5 (+6.25), 412.0 (+2.62), 509.4 (+15.76).

Acetodalmanol B (23). Red crystals, m.p.225−227 °C; UV (MeOH): λ_{max} nm (logε): 509.6 (0.80), 361.6 (1.00), 281.8 (1.26), 247.6 (1.19); IR (KBr) ν_{max}: 3409.3, 2957.3, 1634.8, 1596.3, 1549.0, 1451.2, 1415.7, 1217.6, 1164.5, 1025.7, 989.2, 787.6 cm^{-1}; ^{1}H (500 MHz) and ^{13}C NMR (125 MHz) in DMSO-d_6 see Table 3. HR-ESI-MS: m/z 577.1469 $[M+Na]^+$, calculated for $C_{32}H_{26}O_9Na^+$ 577.1469. (−)-**23**: $[\alpha]^{20}_D$ = −851° (c = 0.01 in MeOH); CD (MeOH): λ_{max} nm ($\Delta\varepsilon$) = 221.3 (−6.89), 247.0 (+13.80), 254.0 (+9.62), 273.4 (+22.00), 292.8 (−23.84), 341.1 (−0.40), 374.8 (−8.21), 425.7 (−0.65), 502.0 (−5.37). (+)-**23**: $[\alpha]^{20}_D$ = +855° (c = 0.01 in MeOH); CD (MeOH): λ_{max} nm ($\Delta\varepsilon$) = 218.9 (+6.61), 247.3 (−13.65), 255.4 (−9.47), 274.1 (−22.90), 292.5 (+24.07), 340.7 (+0.54), 372.5 (+8.25), 422.9 (+0.77), 497.4 (+5.56).

3,4,8-Trihydroxy-6-(hydroxymethyl)-3,4-dihydronaphthalen-1(2H)-one (27). Colorless crystals, mp 168−170 °C; $[\alpha]^{20}_D$ = +38.5° (c = 0.01 in MeOH); UV (MeOH): λ_{max} nm (logε): 332.0 (0.68), 265.0 (1.12), 217.0 (1.32); IR (KBr) ν_{max}: 3399.9, 3166.5, 2906.7,

1647.5, 1557.9, 1430.6, 1340.9, 1306.9, 1258.1, 1193.9, 1066.5, 1027.3, 980.7, 967.2, 858.8, 787.8, 771.4, 689.1 cm^{-1}; CD (MeOH): λ_{max} nm ($\Delta\varepsilon$)= 213.5 (−28.59), 264.6 (+12.70); ^1H (500 MHz) and ^{13}C NMR (125 MHz) in acetone-d_6 see Table S4. HR-ESI-MS: m/z 247.0579 $[M+Na]^+$, calculated for $C_{11}H_{12}O_5Na^+$, 247.0577.

Neocytochalasin (29). Colorless crystals, m.p.197−199 °C; $[\alpha]^{20}_D$ = −81° (c = 0.01 in CH_2Cl_2); UV (MeOH): λ_{max} nm (logε): 381.0 (0.59), 358.0 (0.68), 210.0 (3.29); IR (KBr) ν_{max}: 3351.0, 2962.3, 2929.0, 1701.6, 1681.7, 1458.1, 1433.9, 1378.5, 1366.1, 1299.8, 1157.8, 1092.3, 977.0, 763.1, 620.7 cm^{-1}; CD (MeOH): λ_{max} nm ($\Delta\varepsilon$) = 204.1 (−20.01), 222.2 (+31.86), 297.2 (−10.84); ^1H (300 MHz) and ^{13}C NMR (75 MHz) in $CDCl_3$ see Table S5; HR-ESI-MS: m/z 456.2509 $[M+Na]^+$, calculated for $C_{28}H_{35}NO_3Na^+$, 456.2509.

■ ASSOCIATED CONTENT

Supporting Information. The details of isolation and identification of metabolites, NMR spectra, crystallographic file in CIF format and complete ref 16. This material is available free of charge via the Internet at http://pubs.acs.org.

■ AUTHOR INFORMATION

Corresponding Author
*rxtan@nju.edu.cn

Author Contributions
#Contributed equally to the work.

■ ACKNOWLEDGMENT

Co-acknowledged are the financial supports from MOST (2009ZX09501-013), and NSFC (21072092, 90813036, and 30821006). We also appreciate the fruitful discussions with Prof. D. W. Ma at Shanghai Inst. Org. Chem., Chinese Acad. Sci., P. R. China.

■ REFERENCES

(1) (a) Ge, H. M.; Yang, W. H.; Shen, Y.; Jiang, N.; Guo, Z. K.; Luo, Q.; Xu, Q.; Ma, J.; Tan, R. X. *Chem.—Eur. J.* **2010**, *16*, 6338–6345. (b) Zhang, Y. L.; Ge, H. M.; Zhao, W.; Dong, H.; Xu, Q.; Li, S. H.; Li, J.; Zhang, J.; Song, Y. C.; Tan, R. X. *Angew. Chem., Int. Ed.* **2008**, *47*, 5823–5826.

(2) (a) Scott, J. J.; Oh, D. C.; Yuceer, M. C.; Klepzig, K. D.; Clardy, J.; Currie, C. R. *Science* **2008**, *322*, 63. (b) Oh, D. C.; Poulsen, M. C.; Currie, R.; Clardy, J. *Nat. Chem. Biol.* **2009**, *5*, 391–393. (c) Haeder, S.; Wirth, R.; Herz, H.; Spiteller, D. *Proc. Natl. Acad. Sci. U.S.A.* **2009**, *106*, 4742–4746. (d) Helge, B. B. *Angew. Chem., Int. Ed.* **2009**, *48*, 2–5.

(3) Snyder, S. A.; Sherwood, T. C.; Ross, A. G. *Angew. Chem., Int. Ed.* **2010**, *49*, 5146–5150.

(4) (a) Li, J. W. H.; Vederas, J. C. *Science* **2009**, *325*, 161–165. (b) Ganesan, A. *Curr. Opin. Chem. Biol.* **2008**, *12*, 306–317. (c) Grabowski, K.; Baringhaus, K. H.; Schneider, G. *Nat. Prod. Rep.* **2008**, *25*, 892–904.

(5) Ortholand, J. Y.; Ganesan, A. *Curr. Opin. Chem. Biol.* **2004**, *8*, 271–280.

(6) Crystallographic data have been deposited in the Cambridge Crystallographic Data Centre, as CCDC-791705 (**5**), CCDC-791706 (**6**), CCDC-791707 (**15**), CCDC-791703 (**28**) and CCDC-791704 (**29**). Free copies of the data can be obtained upon application, CCDC, 12 Union Road, Cambridge CB21EZ, UK (fax: (+44)1223−336−033 or e-mail: deposit@ccdc.cam.ac.uk).

(7) (a) Singh, V.; Samanta, B. *Tetrahedron Lett.* **1999**, *40*, 1807–1810. (b) Schuster, D. I.; Kim, C. W. *J. Am. Chem. Soc.* **1974**, *96*, 7437–7444.

(8) (a) Itoh, N.; Katsube, Y.; Yamamoto, K.; Nakajima, N.; Yoshida, K. *Tetrahedron* **2007**, *63*, 9488–9492. (b) Birney, D. M.; Ham, S.; Unruh, G. R. *J. Am. Chem. Soc.* **1997**, *119*, 4509–4517. (c) Schuster, D. I.; Wang, L.; Van der Veed, J. M. *J. Am. Chem. Soc.* **1985**, *107*, 7045–7053.

(9) Rice, J. E.; Cai, Z. W. *J. Org. Chem.* **1993**, *58*, 1415–1424.

(10) Wen, L.; Cai, X.; Xu, F.; She, Z.; Chan, W. L.; Vrijmoed, L. L. P.; Jones, E. B. G.; Lin, Y. *J. Org. Chem.* **2009**, *74*, 1093–1098.

(11) Ayer, W. A.; Browne, L. M.; Lin, G. *J. Nat. Prod.* **1989**, *52*, 119–129.

(12) Wu, Z. C.; Li, D. L.; Chen, Y. C.; Zhang, W. M. A *Hel. Chim. Acta* **2010**, *93*, 920–924.

(13) Scherlach, K.; Boettger, D.; Remme, N.; Hertweck, C. *Nat. Prod. Rep.* **2010**, *27*, 869–886.

(14) Buchanan, M. S.; Hashimoto, T.; Asakawa, Y. *Phytochemistry* **1996**, *41*, 821–828.

(15) Jiemchooroj, A.; Norman, P. *J. Chem. Phys.* **2007**, *126*, 134102/1−7.

(16) Frisch, M. J.; et al. Gaussian 03, Revision D. 01; Gaussian, Inc.: Wallingford, CT, 2004.

(17) Li, J.; Chen, J.; Gui, C. S.; Zhang, L.; Qin, Y.; Xu, Q.; Zhang, J.; Liu, H.; Shen, X.; Jiang, L. *Bioorgan. Med. Chem.* **2006**, *14*, 2209–2224.

(18) He, S.; Wu, B.; Pan, Y.; Jiang, L. *J. Org. Chem.* **2008**, *73*, 5233–5241.